Numerical analysis of snow avalanche mechanics and of its interaction with structures

Eloïse Bovet[1], Bernardino Chiaia[1], Luigi Preziosi[2]
[1]*Department of Structural and Geotechnical Engineering, Politecnico di Torino, Italy*
E-mail: eloise.bovet@polito.it, bernardino.chiaia@polito.it

[2]*Department of Mathematics, Politecnico di Torino, Italy*
E-mail: luigi.preziosi@polito.it

Keywords: Snow avalanche, fluid-structure interaction.

SUMMARY. Two-dimensional models, in the plane parallel to the slope and in the downslope plane, are introduced to describe the avalanche dynamics, and in particular its interaction with obstacles. Their implementation in a FEM software supplies results, that compared with procedures derived empirically, confirm that these models, adequately calibrated, could be used as a support in the design of structures subjected to avalanche impact.

1 INTRODUCTION

The purpose of this paper is to describe a model for the analysis of snow avalanche dynamics and snow-structure interaction. Introducing a procedure used in the design of structures located in avalanche risk area, it is possible to note that the main parameters that a model should calculate are the velocity, pressure, density, depth and volume of the flowing mass.

The Swiss procedure [6] supposes different situations of interference between the avalanche and the structure depending on the position and size of the structure and on the characteristics of the avalanche. For instance, a dense avalanche surrounding a rectangular structure, like a house, reaches an height H given by the contribution of the snow cover (H_s), the depth of the avalanche (H_f) and the height of run up (H_r), due to a loss of a part of the kinetic energy:

$$H = H_s + H_f + H_r = H_s + H_f + \frac{v^2}{2g\lambda} f(\frac{b}{H_f}) \tag{1}$$

As shown in Eq. 1 the last term is characterized by the presence of the empirical dissipation coefficient λ ($1.5 < \lambda < 3$ depending on the kind of the snow) and of the factor ($0.1 < f(\frac{b}{H_f}) < 1$) depending on the ratio between the obstacle width b and the avalanche flow depth: smaller the obstacle is higher the possibility to escape laterally is. Unfortunately, for small obstacles, the last term shows some deficiencies. Let's note that it is supposed that the velocity v is constant along the avalanche depth.

At the heights H_s, H_f and H_r a different load is associated: in the snow cover any forces are transmitted, in the H_f the pressure distribution is uniform, while in the H_r it decreases linearly to 0.

The impact pressure is calculated through the hydraulic relation [10]:

$$p = \frac{1}{2} C_d \rho v^2 \tag{2}$$

where C_d is a drag coefficient, depending on obstacle dimension and shape and on the kind of snow, and ρ is its density. For instance, for the dense avalanche C_d is 1 if the obstacle is narrow, and 2 if it

is large. Even other procedures, as the Norwegian one, apply Eq. 2 with a different range of C_d, that can reaches 6 for a mast. These empirical laws derive from experimental measures.

In the airborne avalanche, instead, C_d is 2 for big obstacles, and it ranges between 1 (circular small obstacle), 1.5 (triangular small ones) and 2 (square small ones). This factor can reaches 6 for very small obstacles. Besides, the interaction between an aerosol and a structure, is compared with the wind effects. The technical regulations concerning the wind actions on structures, in fact, introduce an additional parameter, named the pressure coefficient C_p to relate the values on the different parts of the structure. For instance, [1] proposes for a square of edge L having an area larger than 10 m^2 a factor +0.8 for the upwind side, -0.3 for the downwind one, and a factor varying from -0.8 in the first $L/5$ reached by the flow, to -0.5 in the remaining lateral side. Let's note that these values are quite different in other regulations and take into account of some security factors.

In this paper the features described of these procedures are compared with the results obtained by simulations.

2 THE MODEL

From the Eqs.1-2 it is clear that to design aim it is necessary to know the velocity, pressure, density and depth of the flowing mass. These values are given by a model of avalanche dynamics. In the literature several models have been developed, considering an avalanche only as its centre-of-mass or as a deformable body like a granular material [11] or a fluid, with an hydraulic approach.

In this paper the avalanche is considered a fluid too, but without an integration on the depth. In particular the system constituted by air and avalanche/snow (see Figure 1) is composed by two fluids having different densities and viscosities, and can be modeled by the Navier-Stokes equations:

$$\begin{cases} \nabla \cdot \mathbf{v} = 0 \\ \rho \left(\dfrac{\partial \mathbf{v}}{\partial t} + \mathbf{v} \cdot \nabla \mathbf{v} \right) = \nabla \cdot \underline{\underline{T}} + \mathbf{F} \end{cases} \tag{3}$$

where $\mathbf{v} = (u, v)$ is the velocity, $\underline{\underline{T}} = -p\underline{\underline{I}} + Z(\nabla \mathbf{v} + (\nabla \mathbf{v})')$ is the stress tensor, $\mathbf{F}$ takes into account the gravitational and friction forces (both a Coulomb force and a viscous one), ρ and Z are respectively the density and the viscosity of the air and of the snow.

Let's note that the avalanche itself is considered an incompressible fluid, as almost all the existent models suppose, even if some experimental measures show some change in density.

The NS equations give therefore the values of the velocity and of the pressure in each point of the avalanche.

2.1 *The avalanche depth and volume*

To deduce the value of the depth of the avalanche, that is the H_f in Eq.1, on the contrary of the depth averaged models in which it appears directly in the momentum equation, a further equation have to be introduced.

Let the air-snow interface be described by the material interface $s_2(\mathbf{x}, t) = y - g(x, t) = 0$, and the interface against the underlying motionless snow cover by the function $s_1(\mathbf{x}, t) = y - l(x, t) = 0$. The avalanche depth will be

$$H_f(\mathbf{x}, t) = g(x, t) - l(x, t) \tag{4}$$

It is necessary now to understand how the avalanche/air interface evolves. This interface is assumed to be a material interface for the avalanche. Having normal $\mathbf{n}$ and the initial shape $s_2(\mathbf{x}, t =$

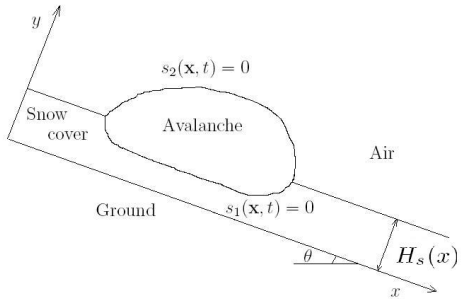

Figure 1: Coordinate system of the 2D-xy model [4].

$0) = 0$, it is transported by the avalanche thanks to the advection equation:

$$\frac{\partial s_2}{\partial t} + \mathbf{v} \cdot \nabla s_2 = 0 \tag{5}$$

Numerically this equation is implemented through the level set method [5], [8], [9]. In fact, the interface $s_2(\mathbf{x}, t)$ can be considered as a level set function characterized to be equal to zero on the the free surface, positive in the zone of the more dense and more viscous fluid (avalanche/ snow) and negative where the less dense and less viscous one (air) is situated. The level set function appears obviously even in the expressions of the density and of the viscosity defined in the whole domain, since they move together with s_2:

$$\rho = \rho_a + H(s_2)(\rho_{av/s} - \rho_a) \tag{6}$$

$$Z = Z_a + H(s_2)(Z_{av/s} - Z_a) \tag{7}$$

where ρ_a (Z_a) and $\rho_{av/s}$ ($Z_{av/s}$) are, respectively, the density (viscosity) of the air and of the avalanche/ snow, and $H(s_2)$ is the Heaviside function.

The boundary conditions, on the interface $s_2(\mathbf{x}, t) = 0$, are the continuity of the velocity, providing the non-penetrability between the air (a) and the avalanche (av) or the snow cover (s):

$$\mathbf{v}_a \cdot \mathbf{n} = \mathbf{v}_{av/s} \cdot \mathbf{n} \tag{8}$$

and the continuity of the normal stress:

$$\underline{\underline{T}}_{av/s} \cdot \mathbf{n} = 0 \tag{9}$$

since $\underline{\underline{T}}_a$ is assumed to be negligible.

The depth of the flow is directly linked with the entrainment of the snow cover too, according to Eq. 4. Entrainment is a phenomenon that significantly affects the avalanche behaviour since it makes a medium/large avalanche increase its mass normally by a factor 2 or 3, where small ones even reach a factor equal to 9 [12]. Recently, some models describing the entrainment have been developed [2], based on different hypothesis, but they are not used practically, due to the lack of experimental data necessary for the validation.

The proposed model [4] describes entrainment, considering the snow cover and the flowing mass, non-Newtonian fluids.

In the case of a Bingham fluid (B) the avalanche is supposed to be in a fluid phase ($I\!I \geq \tau_0^2$):

$$Z_{av} = Z_B = \left(\eta_0 + \frac{\tau_0}{|I\!I|^{1/2}} \right) \tag{10}$$

while the non eroded snow cover results to be in the solid phase ($I\!I < \tau_0^2$):

$$\underline{\underline{\tau}} = G\underline{\underline{B}} \tag{11}$$

where $\underline{\underline{B}}$ is the Cauchy-Green strain tensor, G is the shear modulus, $I\!I$ is the second invariant of the rate of deformation tensor $2\underline{\underline{D}}$, η_0 is the viscosity of the flowing snow and τ_0 the yield stress.

In the shear thinning case (SH) the viscosity has only one expression, namely $Z_{av/s} = Z_{SH}$, in both the avalanche and in the snow at rest:

$$Z_{SH} = \left\{ m|I\!I|^{(n-1)/2} + \frac{\tau_0(1 - \exp(-a|I\!I|^{1/2})]}{|I\!I|^{1/2}} \right\} \tag{12}$$

where m, n, and a are calibration parameters.

Therefore the interface snow cover/avalanche is defined by having the shear stress equal to the threshold value τ_0, i.e.,

$$\mathbf{t'}_{s_1} \cdot \underline{\underline{T}}\mathbf{n}_{s_1} = \tau_0 \tag{13}$$

where $\mathbf{t}_{s_1}$ and $\mathbf{n}_{s_1}$ are respectively the tangential and normal vector at the interface. The interface evolves in time since the zone in which $|I\!I|^{1/2} = \tau_0$ is changed [4].

Hence, the condition of $\tau = \tau_0$ allows to describe which part of the snow cover is entrained by the avalanche, and consequently permits to estimate the total involved volume.

In the simulations presented in this paper, the attention is focused on the interaction between avalanche and structure, and not in the dynamic of the avalanche. For this reason, the interface $s_1(\mathbf{x}, t)$ is characterised by $l(x, t) = 0$, that is there is no entrainment. In fact, we suppose that the entrainment of the snow in the area of the structure studied is negligible. Thereby, in this simplified case, H_f and $g(x, t)$ coincide.

However the more appropriate rheology for the avalanche remains to be determinated. For this goal a possible approach is to compare experimental data with the results of different simulations carried out changing the law of the viscosity [3]. Appropriate laws, like those of the Non-Newtonian fluids in which the viscosity depends on the strain rate, allow to describe correctly the velocity profile along the avalanche depth. Since the velocity and the pressure are linked (see Eq. 2), it is important, for the purpose of correct structural design, to know the pressure profile of the impacting avalanche. However this feature is not taken into account by the majority of the models in the literature, which consider a depth-averaged velocity or give a constant law for the velocity dependence on the depth and neither, as said before, by the Swiss procedure [6]. Since we will compare our results with this procedure, a Newtonian fluid is used.

2.2 *A 2-dimensional model on the XZ-plane*

A different approach is to study the avalanche from above, that is in the XZ-plane (Fig. 2). Even in this situation the system composed by air and avalanche is considered as a fluid. For this reason the same equations of the Navier-Stokes (Eq. 3) and the advection one for the interface air-avalanche $s_3(\mathbf{x}, t) = 0$ (Eq. 5) are used. The notation becomes $\mathbf{x} = (x, z)$ and $\mathbf{v} = (u, w)$.

This model, simpler than an averaged one in which even the depth of the avalanche is taken into account, allows to describe, although roughly, the pressure on an obstacle. The depth of the avalanche, however, can be calculated with the model in 2D on the XY-plane. Finally, since the velocity and the viscosity are considered constant along the depth, in accord with the Swiss Procedure[6], a Newtonian fluid can be used for simplicity.

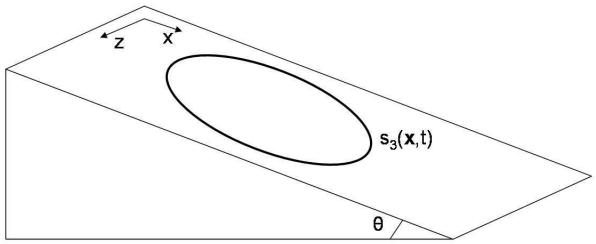

Figure 2: Coordinate system of the 2D-xz model.

3 SIMULATIONS

Once the models for the snow avalanche dynamics has been described, it is possible to simulate the interaction between a snow avalanche and various obstacles located along its path such as, for instance, a concrete dam, an energy transmission pole or a typical masonry house. Simulations were carried out by means of a multiphysics FEM software and, although still qualitative, yields some interesting results.

3.1 *Simulations in 2D on the XY-plane*

A first set of simulations consists in the analysis of the interaction avalanche/obstacle seen from its side. In particular, the simulation reported here analyses the interaction between a dense avalanche and a dam. Fig. 3 shows the pressure along the dam at different time steps. At 1.1s, when the avalanche reaches the dam (Fig. 4.a) there is a peak of pressure, than the upper part of the avalanche reaches the obstacle (Fig. 4.b,c). This behaviour is due to the particular shape (an ellipse) given as initial condition to the avalanche (the lower part arrives before the upper one). In this part of the dam, corresponding to the flowing height H_f the pressure attains the maximal values, in agreement with the Swiss Procedure [6].

In the run-up height H_r, instead, the pressure decreases linearly, according to the Swiss Procedure (see Fig. 3). On the obstacle the pressure doesn't go to 0, because a part of the snow is able to overcome the dam (Fig. 5) carrying with itself part of the kinetic energy and, consequently, of the pressure. Hence such simulations, adequately calibrated, could allow in a design phase, to consider the right pressure and to estimate a more correct volume retained by the dam.

3.2 *Simulations in 2D on the XZ-plane*

A second set of simulations shows from above the interaction between an avalanche and an obstacle having a square and a circular shape with different dimensions. In this situation two scenarios are supposed: an open slope and a channeled one, thanks to appropriate boundary conditions (an

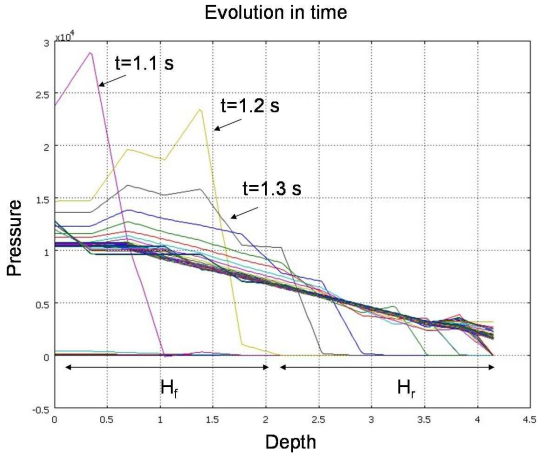

Figure 3: The pressure profile along the obstacle thickness.

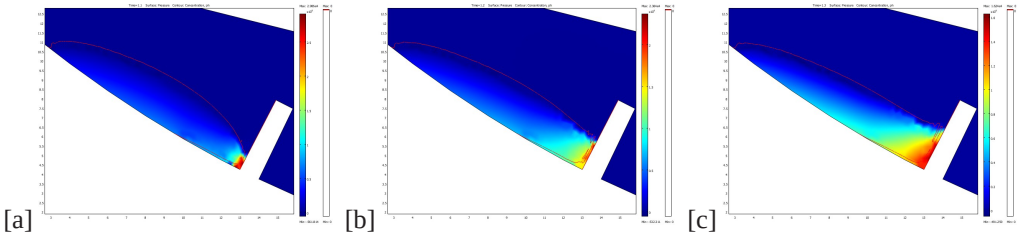

Figure 4: Avalanche pressure on a dam at time 1.1s [a], 1.2s [b] and 1.3s [c] in the flowing height H_f. The range is adapted at each time step to evidence the area with the maximal pressure.

open boundary with normal stress, and a wall with a slip condition). In addition, two densities are supposed to take into account both a dense avalanche (density of about 300 kg/m^3) and an aerosol one (density of 10 kg/m^3).

Simulations show that obstacles having bigger dimensions, both in circular than in the square situation (Fig. 6), split the flow. Qualitatively the fan generated in the impact of the flow is similar to that observed experimentally by [7]. On the contrary, a circular shape of smaller dimension allows to the airborne flow to meet after the obstacle (Fig. 7). A closer study about the dead zone created by the obstacle, for instance, focusing on its size and shape, could be an instrument to conceive efficient passive protection measures, like deflection dams. Besides, an analysis of the deviation of the flow due to obstacles, could explain the formation of different branches created sometimes in the deposit area experimentally observed.

The imposed boundary conditions play an important role when the obstacle has a size comparable with the channel. In fact, an avalanche can expand itself if an open slope is present (Fig. 8.a) or can remain confined if it slides in a channel (Fig. 8.b). Hereby, for practical design even the boundary conditions have to be taken into account. If the obstacle is small, on the contrary, the effects of the

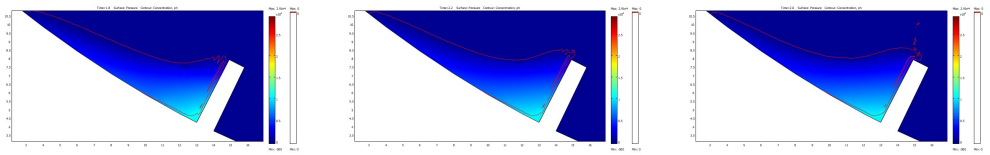

[a] [b] [c]

Figure 5: Avalanche pressure on a dam at time 1.8s [a], 2.2s [b] and 2.8s [c] in the run-up height H_r. The range of the scale is that of the Fig. 4.a.

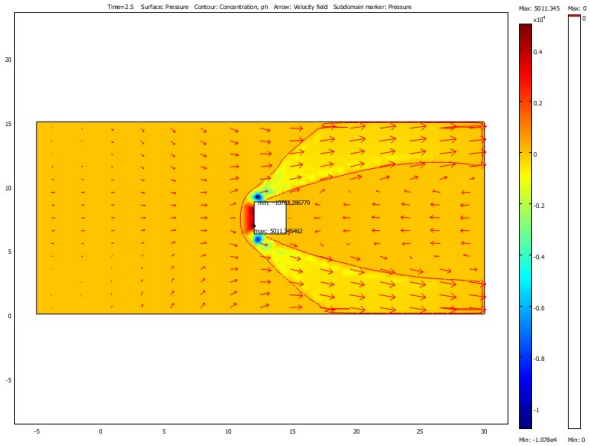

Figure 6: Interaction between a dense avalanche (300 kg/m^3) and a square obstacle in an open slope condition at time 2.5 s. The arrows indicate the velocity, the contour line in red is the interface avalanche-air, the surface plot indicates the pressure.

boundary conditions are less significant (Fig. 9).

The model also allows to calculate the variation in time of the the pressure in a point. For instance, Fig. 10 shows the pressure of the central point upwind a square obstacle: in few seconds (because the avalanche simulated is very small) the avalanche simulated goes beyond the obstacle: the pressure increases quickly and decreases slowly in the avalanche tail. This pressure is compared with the values obtained by the expression 2 in two different ways.

The first one is based on the velocity measured just before the obstacle (in fact, on the obstacle the velocity vanishes for the boundary conditions). For this situation we found a C_d using the maximal values of the velocity and pressure. It's important to underline that the avalanche, in our simulations, has not yet attained a stationary value when it crashes on the obstacle. This aspect can influence significantly the results obtained. In fact, normally in Eq. 2, the pressure is derived from the velocity considering a stationary situation. In addition, for the nature of our simulation that lasts few seconds, the initial phase of the crash plays an important role. On the contrary in the experiences in the wind tunnel the initials steps of the interference are neglected, to consider only the stationary case.

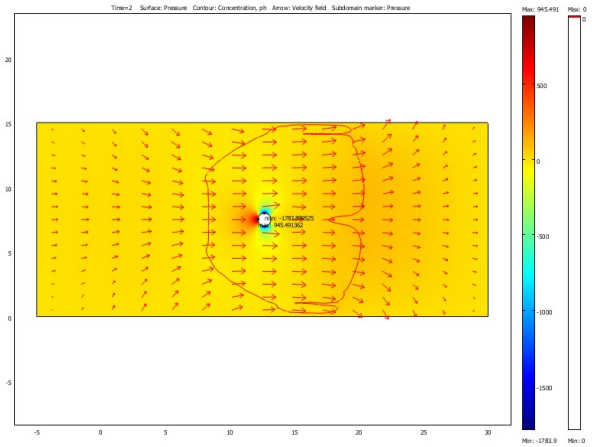

Figure 7: Interaction between an airborne avalanche (10 kg/m^3) and a small circular obstacle in an open slope condition at time 2 s.

A second approach consists in a comparison using the velocity measured in a condition without the obstacle. Fig. 10 shows as the air moved by the avalanche arrives on the obstacle before the avalanche itself and consequently a pressure is measured even before the avalanche without the obstacle arrives in this point. In this situation, having a larger velocity leads to a lower C_d.

Finally, simulations allow to describe the impact pressure of an aerosol avalanche against a building. Fig. 11 shows that on the windward side the pressure is positive, while in the other sides it is negative, similarly to the wind effects.

In this case the C_p are now calculated using the extreme values derived by our simulation: the maximal value is 861 Pa in Fig. 12a, the minimal values -595 Pa in Fig. 12b and -47 Pa in Fig. 12c at the edge centre. Consequently the pressure of impact becomes 1076.7 Pa, considering a pressure coefficient for the frontal edge of 0.8.

As concerns the lateral edge, Fig. 12.b shows as there is a $L/5$ region is which the pressure is higher than in the remaining section. Our C_p obtained is -0.6. This lower value could be given by the fact that there is only a little part of the avalanche impacting on the side, on the contrary of the wind experiences in which the wind recovers the whole tunnel.

To interpret the results obtained in the downwind side, it is important to underline that in such simulation the avalanche does not impact on this side. Hence the pressure is given by the blast: using the air density, the C_p obtained is -0.3 on the obstacle rear.

4 CONCLUSIONS

In this paper two numerical models are described to analyse the interaction between snow avalanche and structures. The results obtained are compared with the Swiss procedure for practical design in avalanche risk areas. The models implemented in a FEM software give interesting results. In a 2-dimensional downhill section, for instance, it reproduces the behaviour of the pressure: it is higher in the zone impacted directly by the flow, and it decreases linearly in the run up area. In the plane of the slope, the values of the C_p found for an airborne avalanche are consistent, as order of magnitude, with the wind effects. Besides it shows the presence of a dead zone at the rear of the obstacle, that

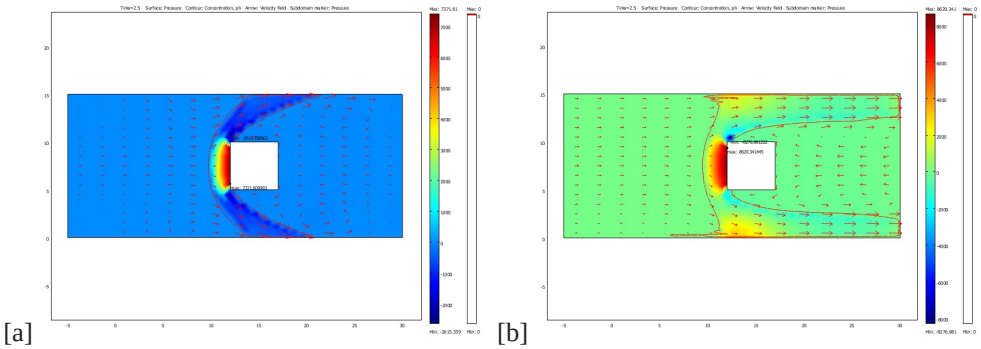

[a] [b]

Figure 8: A dense avalanche in a open slope[a] and in a channel at time 2.5s

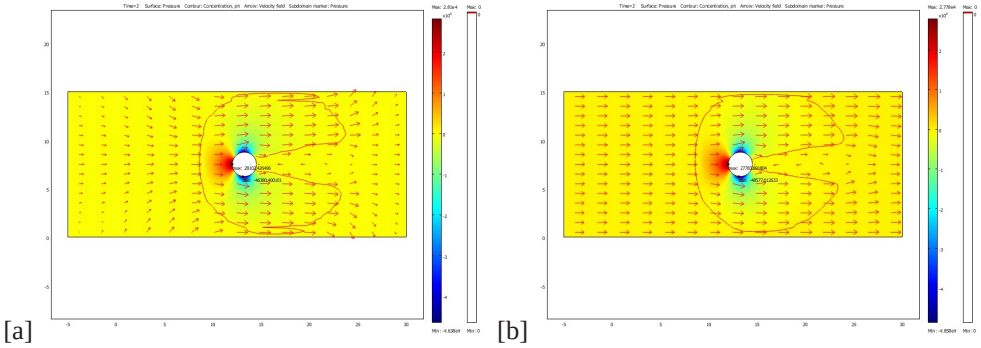

[a] [b]

Figure 9: A dense avalanche in a open slope[a] and in a channel at time 2.0s

is an important aspect for planning purposes. Finally the model allows to find the values of the coefficient C_d in Eq. 2. Let's note that rigorously, to extends these simulations to the real scale of the avalanche, an adimensional analysis must be done, with the introduction of numbers as the Froud's ones and the Reynolds' one.

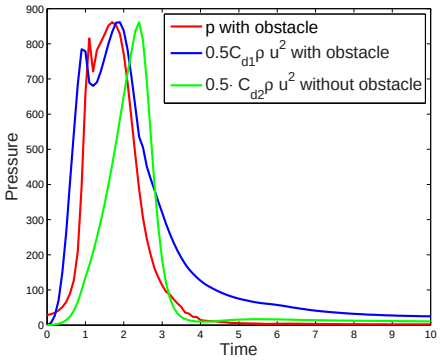

Figure 10: Variation in time of the pressure measured (simulation with the obstacle measured in the point (12,7.5)) and calculated, with the Eq. 2, of the central point upwind of a square hit by an airborne avalanche. $C_{d1} = 0.78$ in the simulation with the obstacle in the point (10,7.5), $C_{d2} = 7.55$ in the simulation without the obstacle in the point (12,7.5))

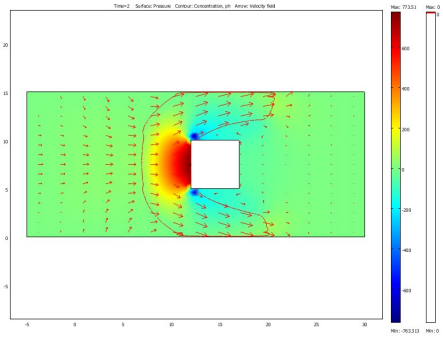

Figure 11: Interaction between an airborne avalanche (10 kg/m^3) and a square obstacle of big dimension in an open slope condition at time 2 s.

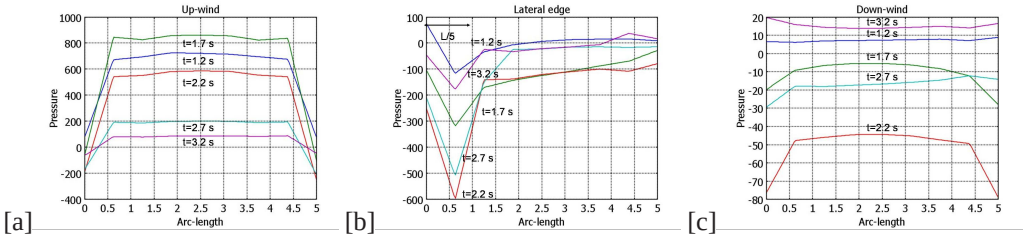

[a] [b] [c]

Figure 12: Avalanche pressure in time up-wind [a], in the lateral edge [b] and down-wind [c].

References

[1] *ENV 1991-2-4:1995. Eurocode 1. Basis of design and actions on structures. Part 2-4: Actions on structures -Wind actions*. 1995.

[2] M. Barbolini, F. Cappabianca, D. Issler, P. Gauer, and M. Eglit. Wp5: Model development and validationerosion and deposition processes in snow avalanche dynamics: report on the state of the art. Technical report, SATSIE PROJECT, 2003.

[3] E. Bovet, B. Chiaia, and L. Preziosi. Test of different rheological models for snow avalanche flow dynamics. *Submitted to Granular Matter*.

[4] E. Bovet, B. Chiaia, and L. Preziosi. A new model for snow avalanche dynamics based on bingham fluids. *Submitted to Meccanica*, 2009.

[5] E. Bovet, L. Preziosi, B. Chiaia, and F. Barpi. The level set method applied to avalanches. *Proceedings of the European COMSOL Conference 2007 in Grenoble, France*, 2007.

[6] T. Egli. *Richtlinie Objektschutz gegen Naturgefahren*. Gebaudeversicherungsanstalt des Kantons St. Gallen, 1999.

[7] S. Hauksson, M. Pagliardi, M.Barbolini, and T. Jóhannesson. Laboratory measurements of impact forces of supercritical granular flow against mast-like obstacles. *Cold Regions Science and Technology*, (49):54–63, 2007.

[8] C. Leppert and D. Dinkler. A two-phase model for granular flows applied to avalanches. *III European Conference on Computational Mechanics Solids, Structures and Coupled Problems in Engineering*, 2006.

[9] S. Osher and J. Sethian. Fronts propagating with curvature dependent speed: Algorithms based on hamilton-jacobi formulations. *Journal of Computational Physics*, 1988.

[10] B. Salm, A. Burkard, and H. Gubler. Berechnung von fliesslawinen: eine anleitung f ur praktiker mit beispielen. Technical report, Institut fédéral pour l'étude de la neige et des avalanches, 1990.

[11] S. Savage and K. Hutter. The dynamics of granular materials from initiation to runout: Part i. analysis. *Acta Mechanica*, (86):201–231, 1991.

[12] B. Sovilla, S. Margreth, and P. Bartelt. On snow entraiment in avalanche dynamics calculations. *Cold Regions Science and Technology*, 2007.